e-ISSN: 2149-4584

Erzincan University Journal of Science and Technology

EJSAT 2026, 19 (1) 253-267

Research Article

Investigation of Fog Harvesting Performance of Functional Thin Film-Coated 3D Surfaces

Meryem Coplan[1], Kurtuluş Yılmaz[1], Emine Sevgili Mercan[1], Mehmet Gürsoy[1*], Mustafa Karaman[1]

[1] Department of Chemical Engineering, Konya Technical University, Campus, Konya 42030, Türkiye

Received: 19/05/2025, **Revised:** 28/10/2025, **Accepted:** 05/11/2025, **Published:** 30/03/2026

Abstract

Access to clean water is one of the major global challenges due to the depletion of natural freshwater reserves, exacerbated by global warming and increasing world population. Reverse osmosis and desalination methods are commonly used for clean water production; however, these methods have high investment and energy costs, limiting their widespread application. In recent years, atmospheric water collection, using fog, has emerged as an energy-efficient, low-cost, and environmentally friendly alternative method. However, traditional fog harvesting nets have low efficiency, prompting increasing interest in developing materials that can collect fog at higher yields. In this study, 3D printing was used to create surfaces with various topographies, which were then coated with hydrophilic polyacrylic acid (PAA) and hydrophobic polyhexafluorobutyl acrylate (PHFBA) thin films in a single step, utilizing the environmentally friendly plasma enhanced chemical vapor deposition (PECVD) technique. Additionally, surfaces exhibiting both hydrophilic and hydrophobic properties were designed and fabricated. The chemical structure, topographical features, and wettability characteristics of the coated surfaces were thoroughly characterized. A total of 22 samples with different surface structures and wettability properties were produced. Fog harvesting experiments revealed that, compared to the control surface, the surface designs achieved up to a 270% increase in fog harvesting efficiency. The results demonstrate that surface topography and wettability are key factors influencing fog harvesting performance.

Keywords: Functional thin film, Fog harvesting, Hydrophilic, Hydrophobic, PECVD

Fonksiyonel İnce Film Kaplı 3B Yüzeylerin Sis Toplama Performansının İncelenmesi

Öz

Temiz suya erişim, doğal tatlı su kaynaklarının tükenmesi, küresel ısınma ve artan dünya nüfusu gibi etkenler nedeniyle, günümüzde karşılaşılan en önemli küresel sorunlardan biridir. Temiz su üretimi için genellikle ters ozmoz ve tuzdan arındırma yöntemleri kullanılmaktadır; ancak bu yöntemler yüksek yatırım ve enerji maliyetlerine sahiptir ve bu durum yaygın kullanımını sınırlamaktadır. Son yıllarda, atmosferik su toplama yöntemi olarak sis kullanımı, enerji verimli, düşük maliyetli ve çevre dostu bir alternatif yöntem olarak öne çıkmaktadır. Ancak, geleneksel sis toplama ağlarının verimliliği düşüktür ve bu durum, daha yüksek verimle sis toplayabilen malzemelerin geliştirilmesine olan ilgiyi artırmıştır. Bu çalışmada, çeşitli topografik yapılara sahip yüzeyler 3D baskı ile üretilmiş ve çevre dostu bir yöntem olan plazma destekli kimyasal buhar biriktirme (PECVD) tekniği kullanılarak, tek adımda hidrofilik poliakrilik asit (PAA) ve hidrofobik poliheksaflorobütil akrilat (PHFBA) ince filmlerle kaplanmıştır. Ayrıca, hem hidrofilik hem de hidrofobik özellikler gösteren yüzeyler tasarlanıp üretilmiştir. Kaplanmış yüzeylerin kimyasal yapısı, topografik özellikleri ve ıslanabilirlik karakteristikleri kapsamlı bir şekilde karakterize edilmiştir. Farklı yüzey yapıları ve ıslanabilirlik özelliklerine sahip toplam 22 örnek üretilmiştir. Sis toplama deneyleri, kontrol yüzeyle karşılaştırıldığında, geliştirilen yüzey tasarımlarının sis toplama veriminde %270'e varan artış sağladığını ortaya koymuştur. Elde edilen sonuçlar, yüzey topografyası ve ıslanabilirliğin sis toplama performansını etkileyen temel faktörler olduğunu göstermektedir.

Anahtar Kelimeler: Fonksiyonel ince film, Sis toplama, Hidrofilik, Hidrofobik, PECVD

Corresponding Author: mgursoy@ktun.edu.tr

Cite this Article: Erzincan University Journal of Science and Technology 2026, 19(1)253-267. https://doi.org/10.18185/erzifbed.1701810

1. Introduction

With the global water crisis becoming increasingly severe, the development of efficient and environmentally sustainable water production techniques has become a critical research priority. Conventional techniques such as reverse osmosis and desalination are widely used but come with significant drawbacks, including high energy demands and the generation of environmentally harmful by-products [1, 2]. These processes typically rely on fossil-fuel-based energy sources, contributing to an increased carbon footprint. As a result, there has been growing interest in alternative water production strategies that are cost-effective, energy-independent, and environmentally sustainable, among which fog harvesting stands out as a promising passive method. Fog harvesting, in particular, offers a passive means of collecting water directly from atmospheric moisture without the need for external energy input. Traditionally, fog harvesting has been carried out using mesh-based fog collectors, but their water yield remains relatively low. To overcome this limitation, researchers have focused on designing advanced materials with improved fog harvesting performance. Notably, many of the most promising fog-harvesting surfaces have drawn inspiration from nature. In nature, organisms such as the Namib Desert beetle, spider webs, and various arid-adapted plant species have evolved highly efficient fog-harvesting surfaces by integrating unique surface geometries and wettability patterns. These natural designs often incorporate hierarchical microstructures, directional grooves, and contrasting hydrophilic-hydrophobic regions to enhance fog harvesting and directional water transport [3–8].

Recent studies highlight the crucial roles of both surface topography and wettability in fog harvesting efficiency. The efficiency of fog harvesting is strongly dependent on surface topography and wettability [9–11]. While existing research has explored micro- and nanostructures, there is limited understanding of how millimeter-scale geometries systematically influence fog harvesting under controlled conditions. Moreover, most studies focus on uniformly hydrophilic or hydrophobic surfaces, overlooking the potential of hybrid wettability configurations. This study aims to address these gaps by presenting a comprehensive investigation of fog harvesting performance across various 3D surface designs. Unlike previous work, our approach integrates diverse geometric configurations including cones, pyramids, cylinders, domes, and cubes, while also exploring the impact of dual wettability, where the surface base and structures exhibit contrasting water affinities. This bilayer design mimics natural systems, where wetting gradients guide water transport from collection to storage regions [12, 13]. To investigate the effects of surface wettability, hydrophilic poly(acrylic acid) (PAA) and hydrophobic poly(hexafluorobutyl acrylate) (PHFBA) thin films were deposited onto the 3D-structured surfaces using plasma enhanced chemical vapor deposition (PECVD). The -OH groups in PAA interact strongly with water droplets, promoting their adsorption and spreading across the surface. In contrast, the fluorine-containing structure of PHFBA imparts low surface energy, leading water droplets to minimize contact, adopt a near-spherical shape, and roll off the surface more easily.

This study aims to evaluate how surface geometry and wettability distribution affect fog harvesting. In total, 22 different surfaces were fabricated, with 12 exhibiting uniform wettability and 10 featuring contrasting wettability between the features and base surfaces. After fabricating these surfaces, fog harvesting performance was systematically tested to assess the impact of surface geometry and wettability on fog harvesting efficiency.

2. Materials and Methods

2.1. Materials

Six distinct surfaces were initially designed using SolidWorks software. The samples were then fabricated using an Artillery Sidewinder-X2 3D printer via fused deposition modeling (FDM), employing polylactic acid (PLA) filament. Each surface was produced with dimensions of 3 cm × 3 cm, and the individual surface features were standardized to a base width and height of 2.4 mm, with a fixed 2 mm spacing between adjacent features. Figure 1 a-f illustrates six surface morphologies: flat, dome shaped, conical, pyramidal, cylindrical and cube shaped, schematically representing the fabricated geometries used in this study.

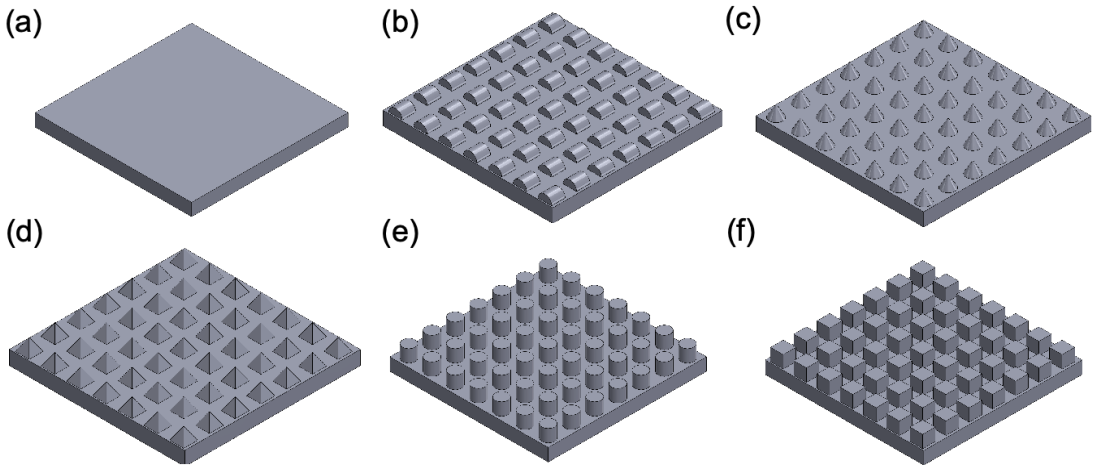

Figure 1. Schematic representation of different micro/nano surface morphologies: (a) flat, (b) dome-shaped, (c) conical, (d) pyramidal, (e) cylindrical, and (f) cube-shaped structures.

To enable the fabrication of geometrically patterned materials exhibiting distinct wettability characteristics on their base and surface structures, additional perforated plates were fabricated. These plates featured openings precisely designed to fit over the surface microstructures without covering them. Functioning as masks, the perforated plates effectively shielded the base regions of the structured substrates, thereby temporarily replacing the original base surfaces during the deposition process. By combining the structured base plates with the perforated masking plates, materials with dual wettability characteristics were successfully produced. The base and surface structures were selectively coated using polymeric thin films with different wetting properties. The overall fabrication strategy involves the integration of distinct surface

features, as illustrated in Figure 2. Specifically, conical microstructures (Figure 2a) and a perforated masking plate (Figure 2b) were combined to form a hybrid structure (Figure 2c). This approach was consistently applied across all surface designs, with the conical geometry serving as a representative example.

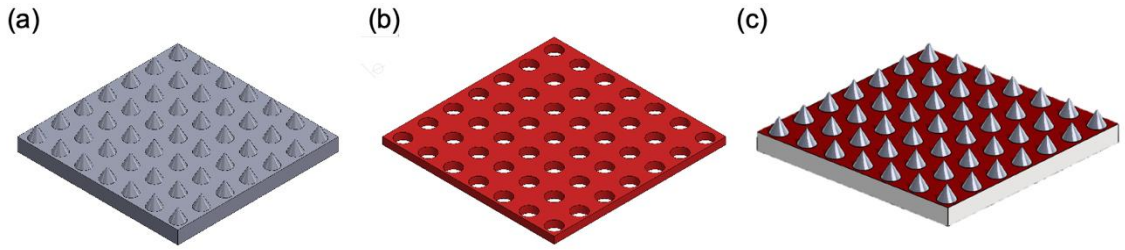

Figure 2. (a) Surface with microstructures, (b) perforated plate, and (c) combined surface incorporating both features. (The same strategy was applied for all surface types; the conical structure is shown as a representative example.)

Including the control sample, a total of 12 samples with uniform wettability, either hydrophobic or hydrophilic, were prepared by coating all surface designs with thin films of a single type. In addition, 10 more samples were fabricated in which the base and surface structures were coated with contrasting wettability properties, such as hydrophilic on the base and hydrophobic on the features, or vice versa. In total, 22 distinct geometrically patterned surface designs were produced by combining various surface structures with different wettability configurations

2.2. PECVD Polymerization

Acrylic acid (AA, 99%, Sigma-Aldrich) monomer was used for hydrophilic coatings, while 2,2,3,4,4,4-hexafluorobutyl acrylate (HFBA, 95%, Sigma-Aldrich) monomer was used for hydrophobic coatings. The chemical structures of both monomers are schematically shown in Figures 3a and 3b, respectively.

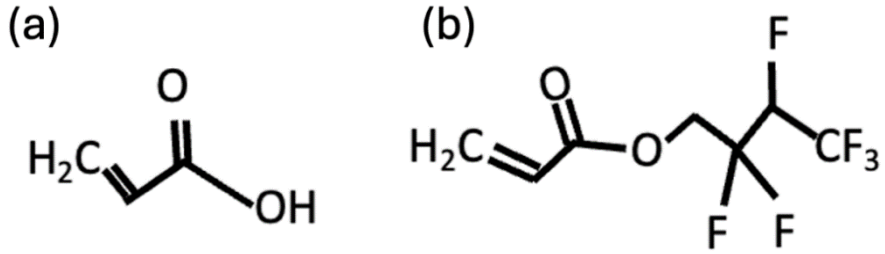

Figure 3. The chemical structures of (a) AA and (b) HFBA

Polymeric thin films were deposited using a custom-built PECVD system. The stainless-steel reactor (15 cm in length and 16 cm in diameter) was equipped with a bottom-mounted heat exchanger connected to a recirculating water bath to control substrate temperature. Detailed specifications of this system have been reported elsewhere [14]. The reactor featured a transparent glass lid, enabling visual monitoring during deposition. Film thickness was

measured in real time using an interferometric system composed of a 632.8 nm laser and a photodetector. A vacuum environment was established with an Edwards XDS-10 vacuum pump, and pressure was monitored using a capacitance manometer. A PID-controlled butterfly valve between the pump and reactor maintained stable operating pressure. Monomers were placed in stainless steel jars and introduced into the reactor via needle valves to control vapor flow rate. A copper antenna positioned above the reactor lid was connected to a 13.56 MHz radio frequency (RF) power supply to initiate plasma polymerization. A matching network was used to ensure efficient power transfer without reflection. Details of the PECVD of PAA and PHFBA deposition experimental conditions were summarized in Table 1.

Table 1. Experimental conditions used for PECVD processes in this study

PECVD parameters	PHFBA	PAA
Plasma power (W)	20	20
Reactor pressure (mTorr)	100	100
Monomer flowrate (sccm)	0,8	1,0
Substrat temperature (°C)	15	15

2.3. Characterizations

The deposition rates were measured during the experiments using a laser interferometer, and after the experiments, with a refractometer. In the laser interferometer measurement, the reflected laser light from the silicon wafer was collected using a detector mounted next to the laser beam. The light intensity was measured with a multimeter connected to the detector. Instantaneous thickness measurements were made using Equation 1, based on the Fresnel Equation and Snell's Law.

$$\frac{d}{fringe} = \frac{\lambda}{2\eta_{polymer}} \quad \text{(Equation 1)}$$

In Equation 1, $n_{polymer}$, λ and d/fringed represent the refractive index of the polymer, the wavelength of the laser light, and the data from the interferogram graph, respectively. The wavelength of the used laser is 632.8 nm. Assuming a refractive index of 1.5 for the polymeric thin film, each d/fringe value in Equation 1 was approximately found to be 211 nm. After completing the experiments, the deposition rates were further confirmed using a refractometer. The chemical analyses of the polymeric thin films were carried out using FTIR and XPS. FTIR was used to identify the functional groups of the polymers, while XPS was employed to determine the elemental composition of the polymers. The FTIR spectra of the polymeric thin films were recorded in the 600-4000 cm^{-1} wavelength range using an FTIR instrument (Thermo Scientific Nicolet iS 10). XPS analysis was performed with a monochromated Al Kα x-ray source (hν = 1486.68 eV) on an XPS (Thermoscientific, K-Alpha, USA) device, using an energy step size of 1 eV at 200 eV, with a 50-second waiting time for the analyses. The wettability of the polymeric thin films was assessed using a goniometer-type contact angle

measurement device (Kruss Easy Drop). Measurements were performed at room temperature using 2 μL of distilled water, with a pH value of around 7.
The surface roughness was measured in a 5 x 5 μm² area using an AFM (TT-2 AFM Workshop) in semi-contact mode. The control surface was analyzed using SEM (Model LS-10, Zeiss) before and after coating with PAA and PHFBA. Prior to SEM analysis, samples were attached to holders using double-sided tape and then coated with approximately 5 nm of gold using a sputter coater (Model 108, Cressington Scientific Instruments Ltd). The fog harvesting performances of the 22 designed samples were tested by exposing them to artificial fog created under controlled laboratory conditions, resembling meteorological fog. The fog harvesting experiments lasted for at least 60 minutes. A custom-built fog generation and collection setup was used for the experiments. Artificial fog was generated using an ultrasonic nebulizer (Pulsemed, Model: GL-2205). The samples were mounted on a beaker placed on an electronic balance and exposed to the fog. Water droplets with diameters between 0.5 and 6.0 μm were delivered to the samples at a flow rate of 300 mL/hour. The distance between the nebulizer and the samples was kept constant throughout all experiments.

3. Results and Discussion

To better understand the interaction between surface morphology and fog harvesting, the geometric parameters of each particle type were quantified. Table 2 presents the total surface area of a single feature, base area of a single feature, fog-exposed surface area of a single feature, total fog-exposed surface area of all features, and the substrate area not occupied by features.

Table 2. Summary of surface area characteristics of the fabricated 3D materials

Samples	Total surface area of a single feature (mm²)	Base area of a single feature (mm²)	Fog-exposed surface area of a single feature (mm²)	Total fog-exposed surface area of all features (mm²)	Substrate area not occupied by features (mm²)
Flat	-	-	-	-	900.00
Cylindrical	27.14	4.52	22.62	1108.38	678.52
Cube-shaped	34.56	5.76	28.80	1411.20	617.76
Pyramidal	18.64	5.76	12.88	631.12	617.76
Conical	14.64	4.52	10.12	495.88	678.52
Dome-shaped	27.16	5.76	21.40	1048.6	617.76

The deposition rates of the polymeric thin films were calculated by dividing the film thickness by the deposition time. The deposition rates of the PAA and PHFBA thin films were determined to be 23 and 15 nm/min, respectively, based on the laser interferometer results. These values were found to be consistent with the results obtained from the reflectometer measurements. FTIR analyses were performed for both thin films. The FTIR spectra of PAA and PHFBA thin films are presented in Figures 4 and 5, respectively. In Figure 4, the main peaks observed in the FTIR spectrum of the PAA thin film are as follows: between 3600-2500 cm^{-1} (COOH

functional group), around 1700 cm^{-1} (C=O stretching), between 1500-1350 cm^{-1} (C-H bending), and between 1300-1100 cm^{-1} (C-O stretching) [15, 16].

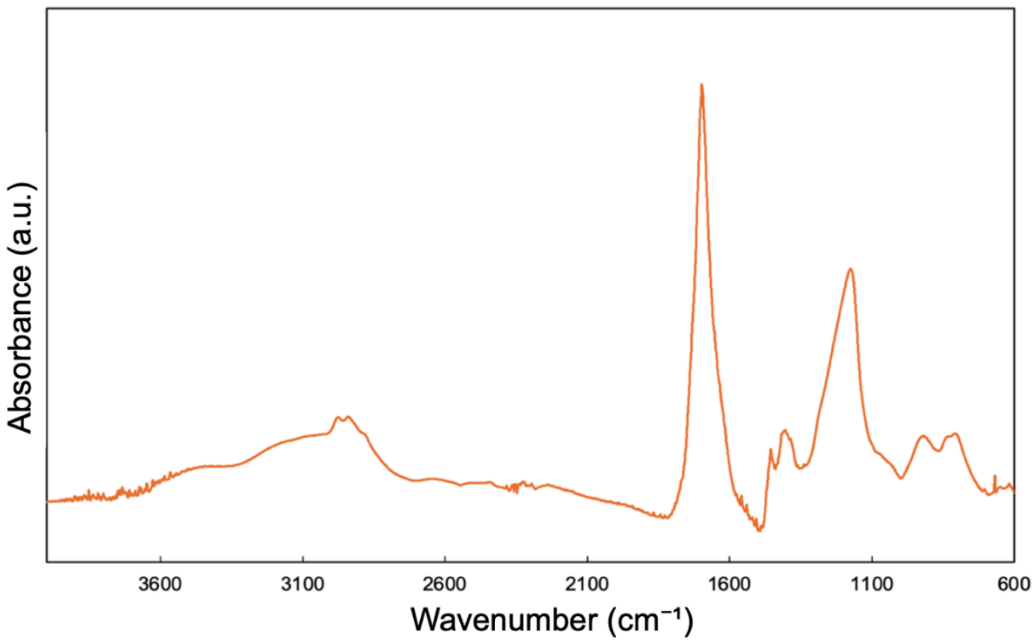

Figure 4. FTIR spectrum of PAA thin film deposited using PECVD

In Figure 5, the main peaks observed in the FTIR spectrum of the PHFBA thin film are as follows: between 3000-2800 cm^{-1} (C-H stretching), around 1740 cm^{-1} (C=O stretching), around 1450 cm^{-1} (CH_2 bending), around 1395 cm^{-1} (CF_3 stretching), around 1290 cm^{-1} (CF_2 vibration), around 1110 cm^{-1} (CFH-CF_3), and around 960 cm^{-1} (CF stretching) [15, 17, 18].

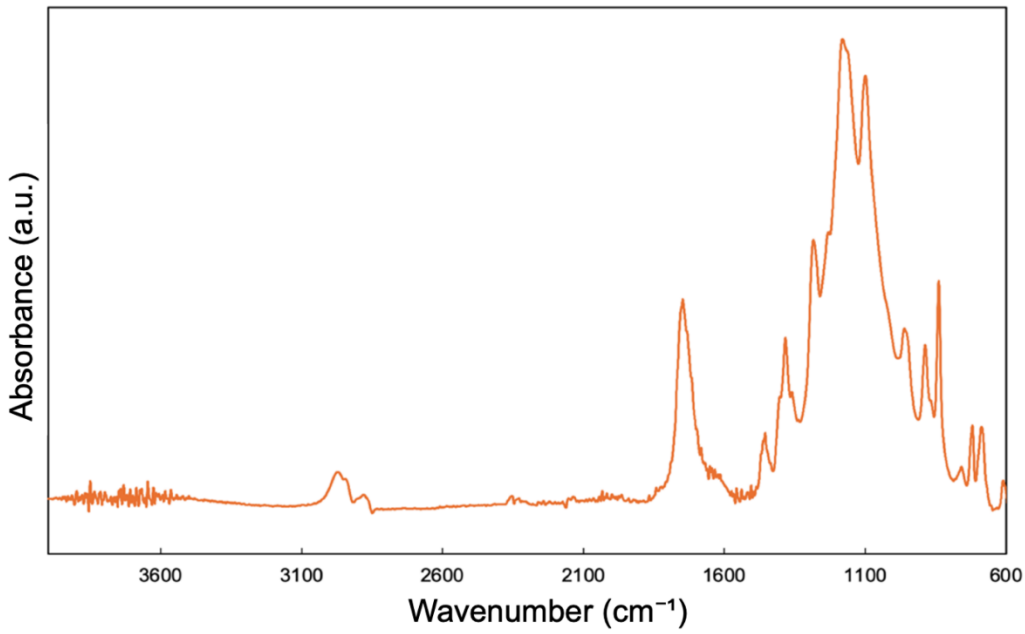

Figure 5. FTIR spectrum of PHFBA thin film deposited using PECVD

In the FTIR spectra of both polymeric thin films, the characteristic C=C double bond peaks typically observed around 1630 cm^{-1} in the spectra of their respective monomers were not detected. The absence of C=C bonds in both polymers indicates that the unsaturated double bonds were successfully reacted during polymerization, confirming the complete conversion of monomers and the absence of residual monomer in the resulting polymer structures.

In addition to FTIR analysis, elemental compositions of the thin films were determined by XPS. As expected, the PAA thin film contained only C and O, while the PHFBA thin film contained only C, O, and F. Elemental analysis revealed that the PAA thin film consisted of 66.1% C and 34.9% O, closely matching the theoretical atomic composition of acrylic acid (60.0% C and 40.0% O). Similarly, the PHFBA thin film was composed of 51.7% C, 11.8% O, and 36.5% F, which is in reasonable agreement with the theoretical atomic composition of HFBA monomer (46.7% C, 13.3% O, and 40% F).

Chemical analyses of the polymeric thin films revealed several noteworthy findings. In the FTIR spectra of both polymers, spectral broadening and increased peak intensities were observed. These features are not considered surprising; in fact, they are commonly encountered in PECVD processes operating in continuous plasma mode, as employed in this study. In such processes, the loss of functional groups and structural alterations may occur due to ion, electron, or neutral species bombardment, or through random recombination of radical groups [19–23]. These effects may also account for the differences between the theoretical and experimentally measured elemental compositions observed in the XPS analysis. Nevertheless, overall, the FTIR results indicate that the functional groups of the monomers were largely preserved, suggesting that the structural integrity of the polymer was maintained throughout the PECVD process.

Contact angle measurements were conducted on uncoated and coated flat 3D surfaces to evaluate the wettability of the films. The images of the water droplets on the uncoated surface, PAA coated surface, and PHFBA coated surface are presented in Figures 6 a, b, and c, respectively. The contact angle of the uncoated sample was measured to be 37.8°, while the PAA coated sample, as expected, exhibited a more hydrophilic nature with a contact angle of 8.1°. In contrast, the PHFBA coated surface demonstrated hydrophobic behavior, with a contact angle of 98.1°, consistent with the nature of the fluorinated polymer. AFM analyses were conducted on the PAA (Figure 6 d) and PHFBA (Figure 6 e) coated silicon wafers to evaluate the roughness of the thin films. For both polymeric coatings, average roughness (Ra) and root mean square roughness (Rq) values were measured. The Ra values were found to be 4.01 nm for the PAA film and 5.70 nm for the PHFBA film, while the corresponding Rq values were 4.95 nm and 6.43 nm, respectively. The findings align with the literature, where smooth polymeric thin films synthesized via CVD methods have been extensively reported [24, 25].

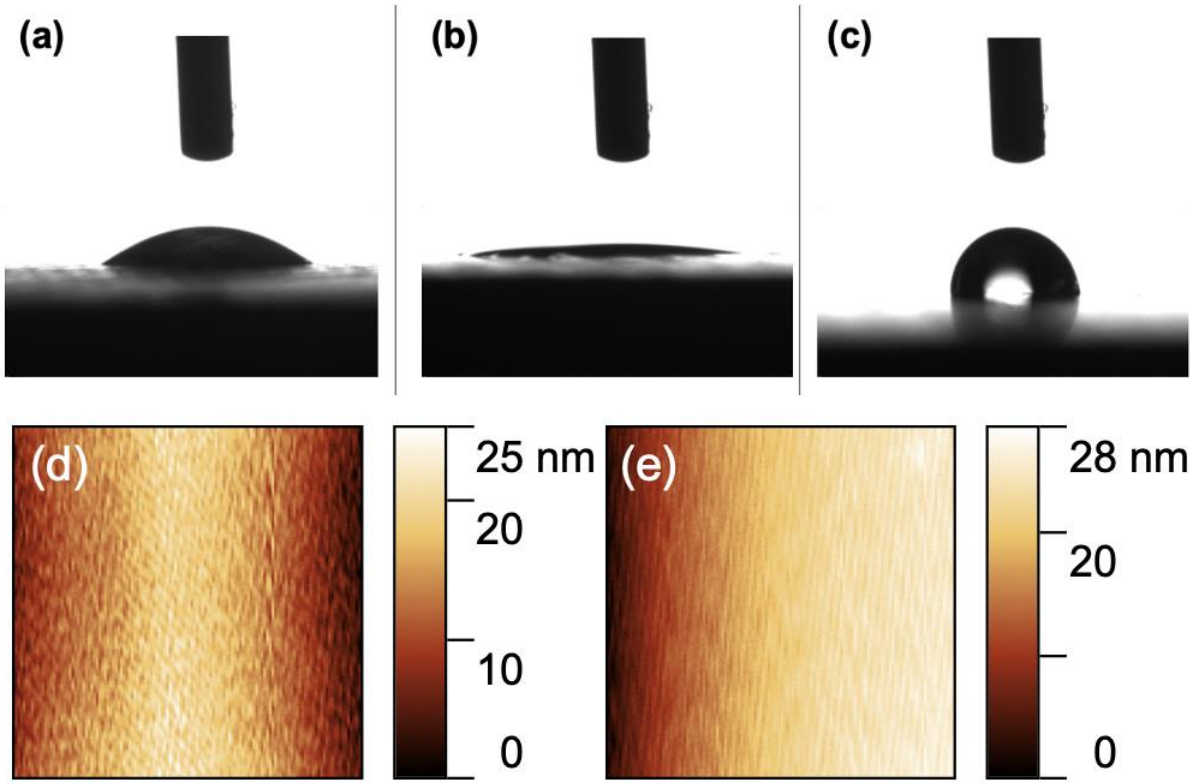

Figure 6. The contact angle images of (a) uncoated, (b) PAA coated, (c) PHFBA coated flat 3D surface. The AFM images of (d) PAA and (e) PHFBA thin film.

The visual appearance of all samples remained unchanged to the naked eye both before and after the coating processes. To enable a more detailed assessment, flat 3D surfaces were examined using SEM. Figure 7 a, b and c presents the SEM images of the uncoated, PAA coated, and PHFBA coated flat 3D surfaces, respectively. No significant differences were observed among the surface morphologies based on the SEM images, indicating that the PECVD coatings did not alter the macroscopic or microstructural appearance of the surfaces.

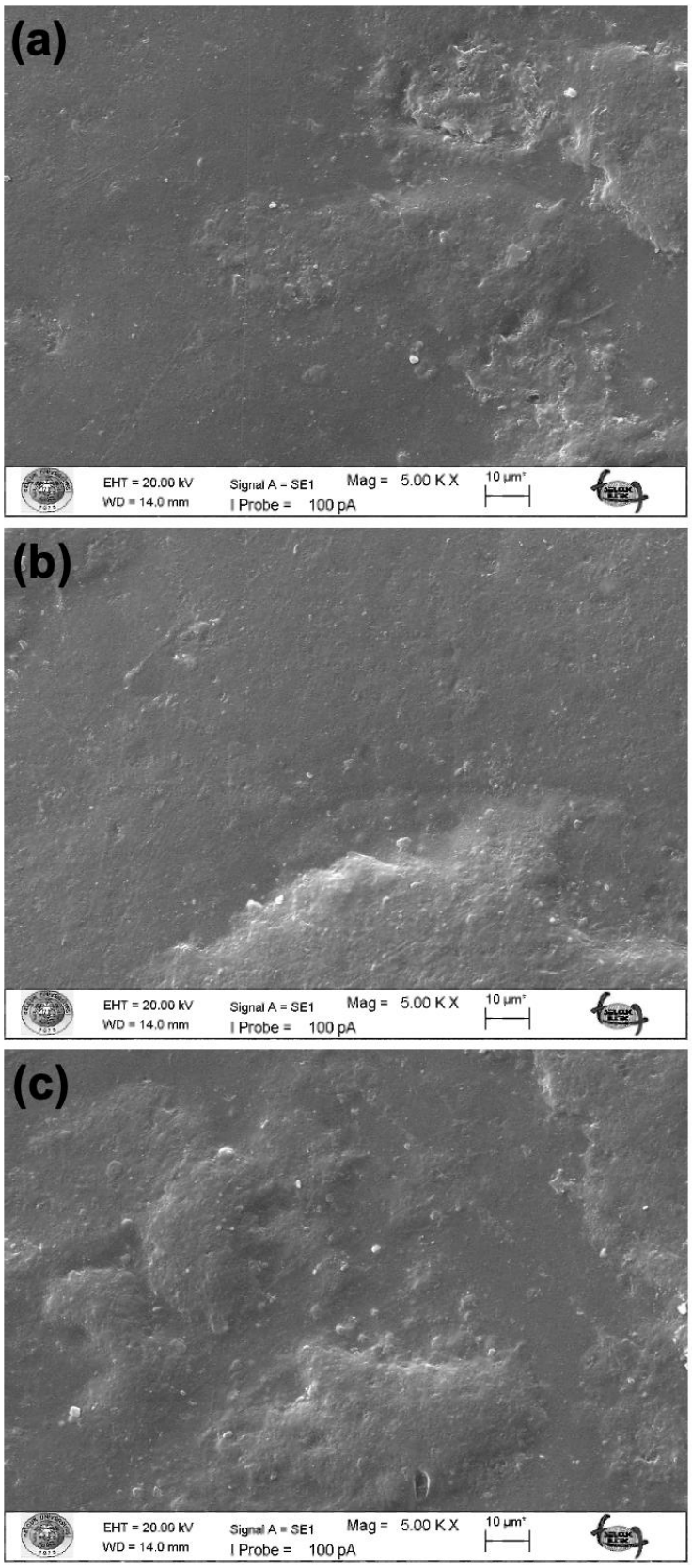

Figure 7. The SEM images of (a) uncoated, (b) PAA coated, (c) PHFBA coated flat 3D surface

The amount of fog harvested by each of the 22 samples over one hour was calculated and is shown in Figure 8.

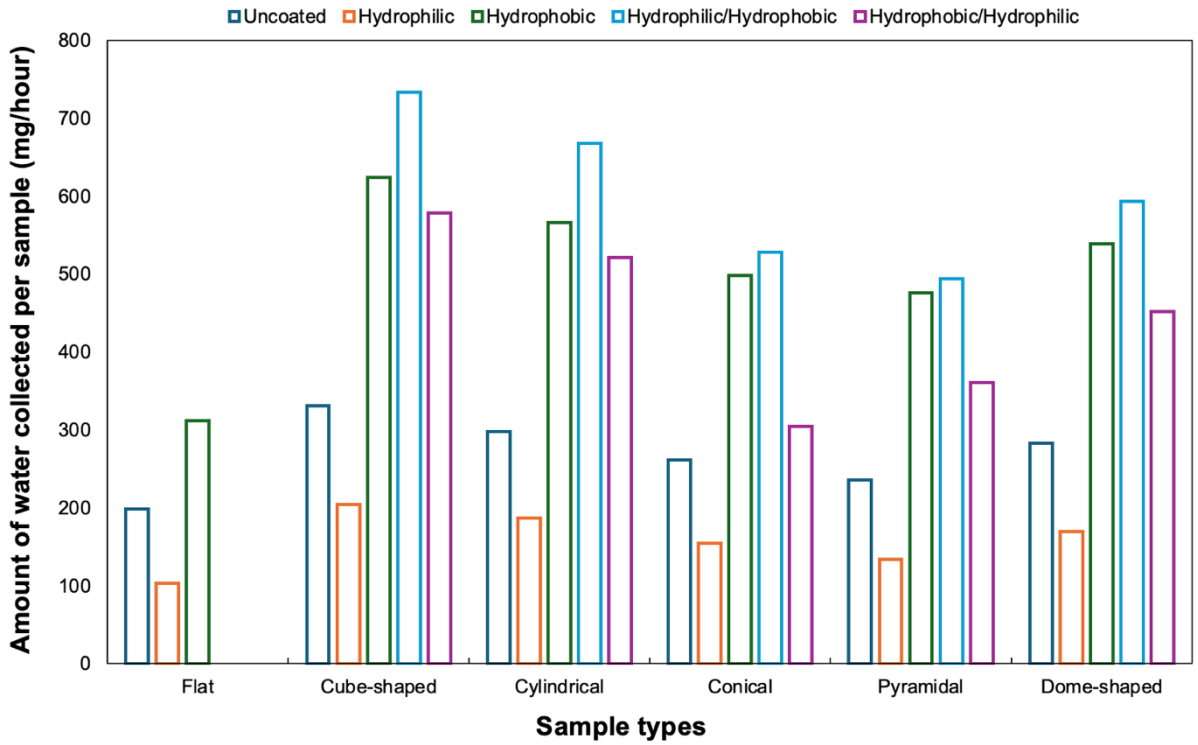

Figure 8. Comparison of fog harvesting performance based on the amount collected per sample

In general, for samples with the same surface geometry, the amount of fog harvested increased in the following order: hydrophilic < uncoated < hydrophobic/hydrophilic < hydrophobic < hydrophilic/hydrophobic. On hydrophilic surfaces, hydrogen bonding occurs between water droplets in the fog and the –OH groups present in the structure of the PAA thin film [26]. These hydrogen bonds promote the adsorption of water droplets onto the PAA coated surface. Due to the strong interaction between water and polar functional groups, the water spreads on the surface. However, the same hydrogen bonding that facilitates adsorption also hinders the detachment of droplets from the surface. Water droplets that cannot detach may either re-evaporate [27] or be carried away by incoming fog vapor, thereby decreasing the number of droplets contributing to downward flow. These mechanisms may decrease the frequency of droplet transport and, consequently, reduce the fog harvesting efficiency of hydrophilic surfaces. In contrast, the relatively more hydrophobic uncoated surfaces may have mitigated the adverse effects associated with hydrophilicity, thereby exhibiting enhanced fog harvesting performance. When fog droplets come into contact with the low-surface-energy PHFBA thin film, they minimize surface interaction due to thermodynamic constraints, adopting near-spherical shapes that promote detachment. This reduces droplet residence time, thereby minimizing re-evaporation and water loss. Consequently, PHFBA coated samples demonstrated superior fog harvesting performance compared to uncoated and hydrophilic samples. Among dual-wettability designs, surfaces with hydrophobic/hydrophilic configurations exhibited slightly lower efficiency than fully hydrophobic ones, likely because droplets detached from the hydrophobic regions before growing large enough to reach the base and be collected. This finding aligns with previous studies reporting that hydrophilic structures combined with a hydrophobic background enhance fog harvesting by facilitating droplet transport and minimizing re-evaporation [28, 29]. This study shows that the combination of hydrophilic

protrusions with a hydrophobic base surface plays a crucial role in enhancing fog harvesting efficiency. Another noteworthy finding regarding fog harvesting performance is the influence of surface geometry. For samples exhibiting identical wettability characteristics, the amount of collected fog increased in the following order: flat < cone < pyramid < dome < cylinder < cube. As anticipated, the presence of surface features significantly enhanced fog harvesting efficiency. A positive correlation was observed between the total surface area contributed by these geometric structures and the collected fog volume. This suggests that increased surface area provides more active sites for droplet nucleation and growth, ultimately improving fog harvesting efficiency. Figure 9 presents the relative improvement in fog harvesting performance for all samples compared to the control sample, i.e., the uncoated flat surface.

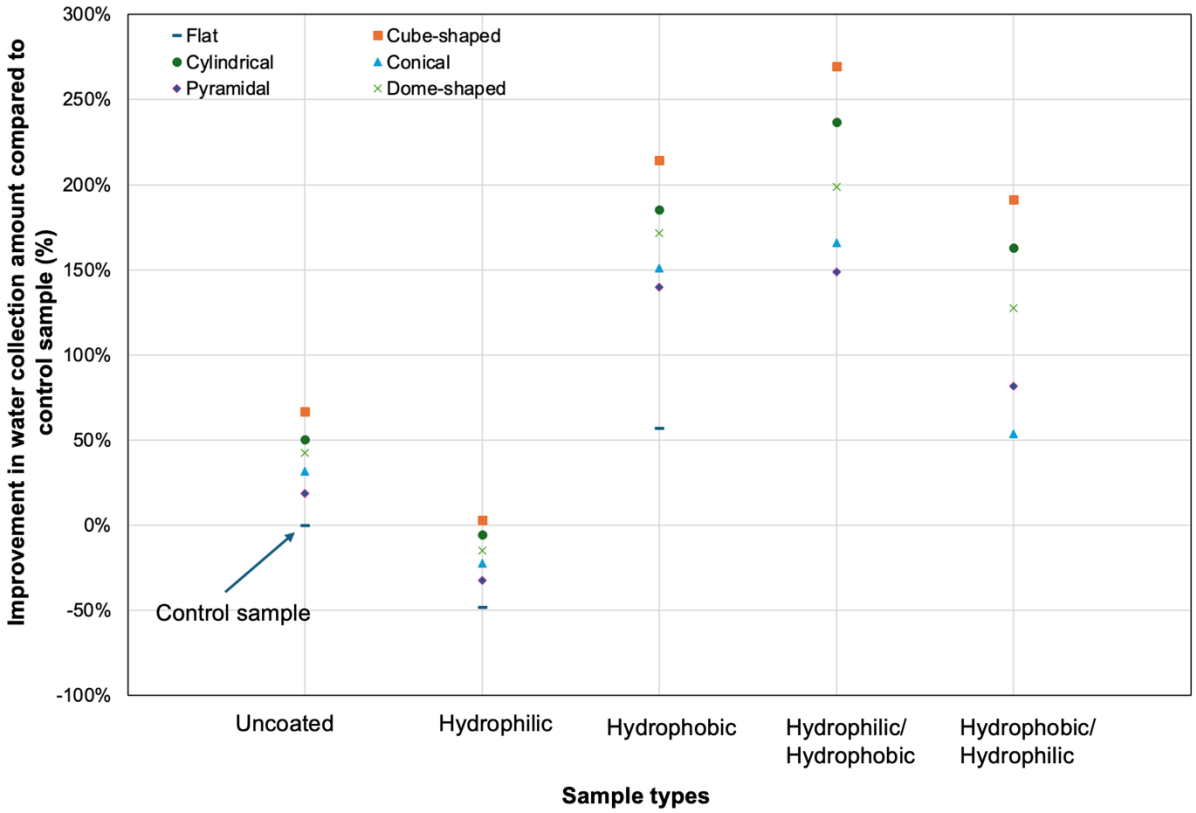

Figure 9. Relative improvement (%) in fog collection efficiency with respect to the control sample

According to the World Health Organization, an individual living under average climatic conditions requires approximately 2.5 liters of clean water per day [30]. In this study, the fog droplets generated by the nebulizer during fog collection experiments were in the range of 0.5–6.0 µm, which closely resembles the droplet sizes typically observed in natural meteorological fog. Among all tested surfaces, the cubic structure with hydrophilic/hydrophobic wettability exhibited the highest fog harvesting efficiency, achieving a 270% increase in collected water compared to the control sample. Based on this result, it can be estimated that a 1 m² surface featuring this design, when exposed to a fog-rich environment for 3 hours, could potentially yield enough water to meet the daily clean water needs of an individual.

4. Conclusions

This study systematically demonstrates that the interplay between surface geometry and wettability distribution significantly influences fog harvesting performance. Among the 22 fabricated surfaces, those combining millimeter-scale 3D structures with dual (hydrophilic/hydrophobic) wettability exhibited the highest collection efficiencies. Notably, cube-patterned surfaces with bilayer coatings outperformed all others, highlighting the synergistic effect of directional droplet transport. These findings provide valuable design principles for the development of efficient, passive water collection systems tailored for arid and fog-prone regions.

Ethics in Publishing

There are no ethical issues regarding the publication of this study.

Author Contributions

M.C., K.Y., E.S: Data curation, investigation and evaluating the results; M.G., M.K.: Funding acquisition, and project administration

Acknowledgements

This study was supported by the Konya Technical University Scientific Research Foundation with a project number of 232216033.

References

[1] Lim, Y. J., Goh, K., Kurihara, M., & Wang, R. (2021). Seawater desalination by reverse osmosis: Current development and future challenges in membrane fabrication – A review, Journal of Membrane Science, 629, 119292.

[2] Voutchkov, N., (2018). Energy use for membrane seawater desalination – current status and trends. Desalination, 431, 2–14.

[3] Li, W., Liu, G., Kong, W., & Jia, H. (2025). Desert Beetle-Like Superhydrophobic/Superhydrophilic TiO_2 –Nanoparticle Patterned Fabric Surface for Fog Harvesting. ACS Applied Nano Materials, 8(6), 2753–2762.

[4] Wang, Q., Tian, G., Zhang, H., He, Y., & Guo, Z. (2025). Hyperphilic/hydrophobic hybridized surfaces for efficient fog harvesting. Journal of Materials Chemistry A, 13(18), 13391–13401.

[5] Hou, L.-L., Qiu, M.-N., Wang, Y.-Q., Bai, T.-H., Cui, Z.-M., Liu, J.-C., … Zhao, Y. (2024). Bioinspired Double-stranded Yarn with Alternating Hydrophobic/Hydrophilic Patterns for High-efficiency Fog Collection. Chinese Journal of Polymer Science, 42(7), 968–975.

[6] Li, M., Xie, S., Tian, G., Chen, G., & Guo, Z. (2024). Biomimetic Leaf-Shaped Wedge Structure with Mixed Wettability for Fog Harvesting. ACS Applied Materials & Interfaces, 16(32), 42931–42941. https://doi.org/10.1021/acsami.4c08254

[7] Wang, J., Guo, Y., Pan, G., Li, Y., Zhang, Y., Yu, H., … Liu, Y. (2022). Hybrid wettability surfaces with hydrophobicity and hydrophilicity for fog harvesting. Colloids and Surfaces A: Physicochemical and Engineering Aspects, 650, 129555. https://doi.org/10.1016/j.colsurfa.2022.129555

[8] Zhang, J., Zhang, Y., Yong, J., Hou, X., & Chen, F. (2022). Femtosecond laser direct weaving bioinspired superhydrophobic/hydrophilic micro-pattern for fog harvesting. Optics & Laser Technology, 146, 107593.

[9] Chakrapani Gunarasan, J. P., & Lee, J.-W. (2024). Active Surface Area-Dependent Water Harvesting of Desert Beetle-Inspired Hybrid Wetting Surfaces. Langmuir, 40(10), 5499–5507.

[10] Showket, J., Majumder, S., Kumar, N., Sett, S., & Mahapatra, P. S. (2024). Fog harvesting on micro-structured metal meshes: Effect of surface ageing. Micro and Nano Engineering, 22, 100236.

[11] Peng, Z., Fu, Y., & Guo, Z. (2023). Origami-like 3D Fog Water Harvestor with Hybrid Wettability for Efficient Fog Harvesting. ACS Applied Materials & Interfaces, 15(31), 38110–38123.

[12] Sun, H., Song, Y., Zhang, B., Huan, Y., Jiang, C., Liu, H., … Wang, H. (2021). Bioinspired micro- and nanostructures used for fog harvesting. Applied Physics A, 127(6), 461.

[13] Kennedy, B. S., & Boreyko, J. B. (2024). Bio-Inspired Fog Harvesting Meshes: A Review. Advanced Functional Materials, 34(35).

[14] Gürsoy, M., Uçar, T., Tosun, Z., & Karaman, M. (2016). Initiation of 2-Hydroxyethyl Methacrylate Polymerization by Tert-Butyl Peroxide in a Planar PECVD System. Plasma Processes and Polymers, 13(4), 438–446.

[15] Lin-Vien, D., Colthup, N. B., Fateley, W. G., & Grasselli, J. G. (1991). The handbook of infrared and Raman characteristic frequencies of organic molecules. Elsevier.

[16] Yılmaz, K., Gürsoy, M., & Karaman, M. (2021). Vapor Deposition of Transparent Antifogging Polymeric Nanocoatings. Langmuir, 37(5), 1941–1947.

[17] Zhang, Y., Yan, Y., Wang, Y., Li, Y., Wang, X., Zhang, H., … Wang, F. (2013). The synthesis and solution properties of hyperbranched polyglycerols modified with hexafluorobutyl acrylate. Colloids and Surfaces A: Physicochemical and Engineering Aspects, 436, 563–569.

[18] Gürsoy, M., & Karaman, M. (2016). Hydrophobic coating of expanded perlite particles by plasma polymerization. Chemical Engineering Journal, 284.

[19] Badyal, J. P. (2001). Beyond the surface-Cold plasmas are streamlining the surface coatings industry. Chemistry in Britain, 37(1), 45–46.

[20] Gürsoy, M. (2020). Fabrication of Poly(N-isopropylacrylamide) with Higher Deposition Rate and Easier Phase Transition by Initiated Plasma Enhanced Chemical Vapor Deposition. Plasma Chemistry and Plasma Processing, 40(4).

[21] Truica-Marasescu, F., Jedrzejowski, P., & Wertheimer, M. R. (2004). Hydrophobic Recovery of Vacuum Ultraviolet Irradiated Polyolefin Surfaces. Plasma Processes and Polymers, 1(2), 153–163.

[22] Vasudev, M. C., Anderson, K. D., Bunning, T. J., Tsukruk, V. V., & Naik, R. R. (2013). Exploration of Plasma-Enhanced Chemical Vapor Deposition as a Method for Thin-Film

Fabrication with Biological Applications. ACS Applied Materials & Interfaces, 5(10), 3983–3994.

[23] Rupper, P., Vandenbossche, M., Bernard, L., Hegemann, D., & Heuberger, M. (2017). Composition and Stability of Plasma Polymer Films Exhibiting Vertical Chemical Gradients. Langmuir, 33(9), 2340–2352.

[24] Abessolo Ondo, D., Loyer, F., Werner, F., Leturcq, R., Dale, P. J., & Boscher, N. D. (2019). Atmospheric-Pressure Synthesis of Atomically Smooth, Conformal, and Ultrathin Low- k Polymer Insulating Layers by Plasma-Initiated Chemical Vapor Deposition. ACS Applied Polymer Materials, 1(12), 3304–3312.

[25] Zhao, Y., Huo, N., Ye, S., & Tenhaeff, W. E. (2023). Elastic broadband antireflection coatings for flexible optics using multi-layered polymer thin films. Journal of Materials Chemistry C, 11(12), 4005–4016.

[26] Ozden, S., Ge, L., Narayanan, T. N., Hart, A. H. C., Yang, H., Sridhar, S., … Ajayan, P. M. (2014). Anisotropically Functionalized Carbon Nanotube Array Based Hygroscopic Scaffolds. ACS Applied Materials & Interfaces, 6(13), 10608–10613.

[27] Bai, H., Wang, L., Ju, J., Sun, R., Zheng, Y., & Jiang, L. (2014). Efficient Water Collection on Integrative Bioinspired Surfaces with Star-Shaped Wettability Patterns. Advanced Materials, 26(29), 5025–5030.

[28] Gürsoy, M. (2020). All-dry patterning method to fabricate hydrophilic/hydrophobic surface for fog harvesting. Colloid and Polymer Science.

[29] Gürsoy, M., & Kocadayıoğulları, B. (2023). Environmentally Friendly Approach for the Plasma Surface Modification of Fabrics for Improved Fog Harvesting Performance. Fibers and Polymers, 24(10), 3557–3567.

[30] Reed, R., Godfrey, S., Kayaga, S., Reed, B., Rouse, J., Fisher, J., … Odhiambo, F. (2013). Technical notes on drinking-water, sanitation and hygiene in emergencies. Loughborough University.